

MASTER

Nitrilation of oleic amide in batch and continuous systems

Hu, Yongli

Award date:
2021

[Link to publication](#)

Disclaimer

This document contains a student thesis (bachelor's or master's), as authored by a student at Eindhoven University of Technology. Student theses are made available in the TU/e repository upon obtaining the required degree. The grade received is not published on the document as presented in the repository. The required complexity or quality of research of student theses may vary by program, and the required minimum study period may vary in duration.

General rights

Copyright and moral rights for the publications made accessible in the public portal are retained by the authors and/or other copyright owners and it is a condition of accessing publications that users recognise and abide by the legal requirements associated with these rights.

- Users may download and print one copy of any publication from the public portal for the purpose of private study or research.
- You may not further distribute the material or use it for any profit-making activity or commercial gain

Nitrilation of oleic amide in batch and continuous systems

Master Thesis

Author: Yongli Hu
Department of Sustainable Process Engineering
Eindhoven University of Technology
y.l.hu@student.tue.nl

Project supervisor: Carola Raffel
c.m.raffel@tue.nl

Graduation supervisor: John van der Schaaf
j.vanderschaaf@tue.nl

Period of master project: 02 November 2020 - 20 July 2021

Last updated on 12 July 2021, Eindhoven

Summary

Nitriles are cyano-substituted organic compounds and are widely used in the chemical and pharmaceutical industry. For example, they can be used in the production of various polymers, solvents, drug intermediates and pesticides.^[1-3] In addition, the ease with which the nitrile group can be converted in other functional groups makes them a commercially important base chemical. For example, hydrogenation of these nitriles can lead to the production of amines which are commonly used as surfactants.^[2] One of the interesting methods, in terms of renewability/sustainability, is to produce nitriles from non-edible biomasses.^[1-4]

This method can use the non-edible triglycerides from animal or vegetable fats, e.g. lard, tallow coconut, palm and peanut oils, to obtain fatty acids.^[1,2,4] The reaction mechanism of fatty nitriles from fatty acids have not been studied extensively, neither in batch nor in continuous systems. Therefore a kinetic study is done on the reaction of the intermediate, oleic amide, into oleic nitrile. During this project, the liquid phase reaction will be studied in batch and continuous systems. Therefore, the main goal of this project is to conduct a kinetic study on the liquid phase reaction mechanism of oleic amide into oleic nitrile and oleic nitrile in batch and continuous systems.

To achieve this goal, the thesis has been structured into the following sub-goals listed below.

- Studying the reaction mechanism of oleic amide in a batch and continuous system.
 - Constructing a continuous plug flow reactor for the nitrilation reaction.
 - Studying the effect of various reaction conditions on the systems such as reaction time, temperature, and composition.
- Obtaining kinetic and thermodynamic parameters from the reaction.
 - Obtaining kinetic parameters such as reaction rate constants, reaction orders, activation energy and pre-exponent constant.
 - Obtaining thermodynamic parameters as enthalpy and, entropy.
- Comparing the batch and continuous systems to evaluate which system performs better.

During this thesis, a batch reactor was used to study the reactions of oleic amide. Due to the constant purge of water and ammonia, full conversion could be reached at long reaction times. Also, the effects of temperature were investigated at which a higher temperature improved the conversions of amide but also increased the amount of side reactions happening thus lowering the overall nitrile yield. At a conversion of 90 %, the highest nitrile yield that was achieved was 60 % at 300 °C. Furthermore, it is shown that side reactions are most likely happening with the unsaturated bonds in the carbon chains. At last, evidence is shown that water could have a mass transfer limitation in the liquid phase.

Also, a continuous plug flow reactor was used to study the reactions with oleic amide at different temperatures. With the use of the experimental data, a theoretical model has been constructed using Matlab from which the reaction rate constants and order could be estimated. The experimental data shows an equilibrium state and closely resemble the theoretical model. Because equilibrium states were observed, the highest conversion that was seen was at 55 % after 25 minutes along with a nitrile yield of 29 %. Therefore, the continuous system performed worse in comparison with the batch setup.

As for the Arrhenius constants, negative activation energies were calculated which is not possible for these reactions and a better model has to be constructed to estimate the k-values more accurately.

Finally, the enthalpy and entropy of the reaction have been calculated. It is shown that the first reaction is slightly exothermic with an enthalpy of -16.9 kJ/mol and entropy of -37.36 J/mol. As for the second reaction, the reaction is highly endothermic with an enthalpy of 168 kJ/mol and entropy of 276 J/mol.

Table of contents

Summary	1
List of Figures.....	3
List of Tables.....	3
List of Abbreviations.....	4
1. Introduction.....	5
2. Theoretical background.....	6
2.1 Literature review	6
2.2. Kinetic parameters	7
2.2. Operational systems.....	9
2.3. Gas chromatography	10
3. Experimental	11
3.1. Materials.....	11
3.2. Method.....	12
4. Results	15
4.1. Batch system	15
4.2. Investigation of product losses in oleic compounds	17
4.3. Continuous system	19
4.4. Arrhenius plot.....	22
4.5. Van 't Hoff plot	23
5. Conclusion and recommendations.....	24
5.1. Conclusion	24
5.2. Recommendations	26
References.....	27
Appendix I: Matlab files.....	29
Appendix II: GC-MS analysis of oleic amide	32
Appendix III: Molecular sieves in the batch reactor.....	33

List of Figures

Figure 1: General illustration of the Arrhenius plot	8
Figure 2: General illustration of the Van 't Hoff plot of an exothermic reaction	8
Figure 3: Diagram of a gas chromatograph	10
Figure 4: Schematic of the batch setup	12
Figure 5: Schematic of the flow setup	13
Figure 6: Concentration profiles of oleic nitrile, acid and amide and temperature profile at 300 °C in the batch setup	15
Figure 7: Concentration profiles of oleic nitrile, acid and amide and temperature profile at 270 °C in the batch setup	16
Figure 8: Concentration profile of oleic compounds at 330 °C in the batch setup	16
Figure 9: Loss of oleic compounds at different reaction temperatures	17
Figure 10: Effect on the concentration profiles with condenser (C) and without condenser (NC)	18
Figure 11: Concentration profile of lauric compounds at different temperature ranges	19
Figure 12: Concentration profile of oleic compounds at 300 °C in the flow setup at which the theoretical model is denoted as (T) and the experimental data as (E).	20
Figure 13: Concentration profile of oleic compounds at 270 °C in the flow setup at which the theoretical data is denoted as (T) and the experimental data as (E).	21
Figure 14: Concentration profile of oleic compounds at 250 °C in the flow setup at which the theoretical data is denoted as (T) and the experimental data as (E).	21
Figure 15: Arrhenius plot of the different reactions	22
Figure 16: Van 't Hoff plot of the reactions	23
Figure 17: Initial test with molecular sieves	33

List of Tables

Table 1: Materials	11
Table 2: Equipment	11
Table 3: Results of the Arrhenius plot	22
Table 4: Results of the Van 't Hoff plot	23
Table 5: GC-MS analysis of oleic amide	32

List of Abbreviations

A	Pre-exponential factor
ΔG	Gibbs free energy
ΔH	Enthalpy
ΔS	Entropy
E_a	Activation energy
FID	Flame ionization detector
GC	Gas chromatography
GC-MS	Gas chromatography – Mass spectrometry
K_{eq}	Equilibrium constant
k_i	Reaction rate constant
PFR	Plug flow reactor
R	Ideal gas constant
r_i	Reaction rate
T	Temperature

1. Introduction

Nitriles are cyano-substituted organic compounds and are widely used in the chemical and pharmaceutical industry. For example, they can be used in the production of various polymers, solvents, drug intermediates and pesticides.^[1-3] In addition, the ease with which the nitrile group can be converted in other functional groups makes them a commercially important base chemical. For example, hydrogenation of these nitriles can lead to the production of amines which are commonly used as surfactants.^[2] Nitriles can be prepared via various different methods, including metatheses of organohalides, ammoxidation of hydrocarbons and addition of hydrogen cyanide to unsaturated organic compounds such as aldehydes, ketones and olefins. One of the interesting methods, in terms of renewability/sustainability, is to produce nitriles from non-edible biomasses.^[1-4]

This method can use the non-edible triglycerides from animal or vegetable fats, e.g. lard, tallow coconut, palm and peanut oils, to obtain fatty acids.^[1,2,4] These fatty acids can further react into a fatty amide which can then consecutively react into a fatty nitrile group. The reaction mechanism of fatty nitriles from fatty acids have not been studied extensively, neither in batch nor in continuous systems. Therefore a kinetic study is done on the reaction of the intermediate, oleic amide, into oleic nitrile. During this project, the liquid phase reaction will be studied in batch and continuous systems.

Therefore, the main goal of this project is to conduct a kinetic study on the liquid phase reaction mechanism of oleic amide into oleic nitrile and oleic nitrile in batch and continuous systems.

To achieve this goal, the thesis has been structured into the following sub-goals listed below.

- Studying the reaction mechanism of oleic amide in a batch and continuous system.
 - Constructing a continuous plug flow reactor for the nitrilation reaction.
 - Studying the effect of various reaction conditions on the systems such as reaction time, temperature, and composition.
- Obtaining kinetic and thermodynamic parameters from the reaction.
 - Obtaining kinetic parameters such as reaction rate constants, reaction orders, activation energy and pre-exponent constant.
 - Obtaining thermodynamic parameters as enthalpy and, entropy.
- Comparing the batch and continuous systems to evaluate which system performs better.

The relevant theory of this project has been summarized in chapter 2. From this, a method is formed in chapter 3. Chapter 4 includes the results and discussion of the project. From this, a conclusion will be drawn in chapter 5 and several recommendations will be made in chapter 6. All the experiments have been performed with the materials and equipment at the laboratories of the Sustainable Process Engineering group at the Eindhoven University of Technology during a nine months graduation project.

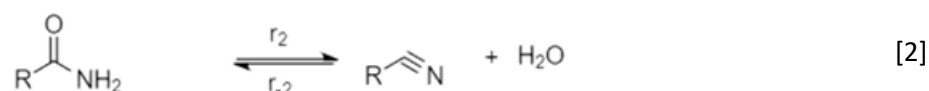
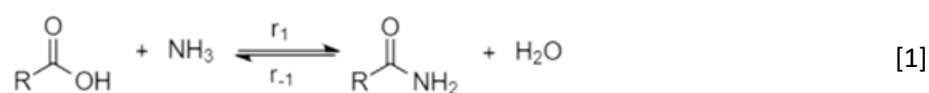
2. Theoretical background

2.1 Literature review

As previously mentioned, the reaction mechanism of fatty acids into fatty nitriles has not been investigated extensively but there are several literature sources which do focus on this topic. In this chapter, several literature topics are summarized which include the reaction mechanism, liquid phase and gaseous phase reaction.

Reaction mechanism

The nitrilation reactions from fatty acids to fatty nitriles can either take place in liquid phase or can be vaporized and can take place in the gaseous phase. The reaction mechanisms for both the liquid as well as the gaseous phase behave similarly and the reactions can be separated into two consecutive reactions, which can be seen in equation 1 and 2 (where, $R = C_{17}H_{33}$ for oleic compounds).^[2] The first reaction is a reversible amidification reaction between the carboxylic acid and ammonia to produce an amide and water. The second reaction is a reversible nitrilation reaction of amide into nitrile and water.



Additionally to the two reactions, several side reactions could occur e.g. isomerization, polymerization, Piria, Diels-Alder or peroxidation reactions. A couple of papers have reported the possibilities for these reaction and point out that these reactions particularly happen in the presence of unsaturated fatty acids, but none of which discussed the rates at which these reactions occur.^[1,2,4]

Liquid phase reaction

In 1985, Bizhanov et al. researched the kinetics of the nitrilation reaction of aliphatic acids. During their research, a mixture of nitriles was synthesized in a packed bed flow reactor at steady state from C_{12} to C_{22} aliphatic acids at 300 °C using aluminium oxide as catalyst and with a continuous stream of ammonia. They stated that there is another intermediate reaction at which the carboxylic acids first react with ammonia into a salt which consecutively reacts to the amide, but no reaction mechanism is shown to support this statement and only small weight percentages were observed (< 2 wt %). They were able to reach a full conversion after 2 hours while achieving nitrile yields up to 98 %. They also claimed that the reaction order of acid and amide are zero-order and that these concentrations do not affect the reaction rates which is improbable. The rates at which they were able produce amide and nitrile are equal to 7.4 and 5.88 mol/min, respectively.^[5]

From this, Mekki-Berrada et al. (2013) conducted their own research in which they studied the reaction of fatty acid into fatty nitriles using heterogeneous or homogeneous or no catalyst. In the reactions without any catalyst, they studied the reaction kinetics at 300 °C using oleic amide in a closed batch reactor. During the experiments with oleic amide without a continuous ammonia stream, they found that the reaction mixture eventually reaches an equilibrium after 3.5 hours with a 5:35:60 repartition of amide, acid, and nitrile, respectively. They also conducted an experiment using oleic nitrile with water at which they found no conversion towards amide and concluded that the secondary reaction is not reversible. This is contradicting to the fact that they found an equilibrium state in their previous experiments. Furthermore, they calculated the reaction rate constants implicitly at 300 °C and found rate constants of 0.725, 0.090, and 0.150 h⁻¹ for the first forward reaction, first backwards reaction and

second forward reaction, respectively. Due to lack of knowledge on the exact composition, their calculation were under the assumption that the order of the reactions are of first order, acid will only exist as an ammonium-salt and that water concentration can be treated as a constant.^[1]

In the paper of Shirazi et al. (2017), an experiment with coconut oil was shown, which mainly consist of C₁₂ to C₁₈ aliphatic acids, in the liquid phase and without catalyst. This experiment was done in a plug flow reactor at 300 °C with low residence times (10 minutes) and were able to calculate the energy required for this reaction. They stated that the nitrile production at this temperature requires 387 kJ/kg triglyceride which equals to 271.16 kJ/mol acid.^[2]

Gaseous phase reaction

As previously mentioned, the reactions can either take place in a gaseous or liquid phase reaction. According to Mekki-Berrada^[1], the two reactions have different kinetics at which the gas phase reaction is faster but has a lower selectivity towards the nitrile than the liquid phase reaction and the liquid phase reaction is slower but has a higher selectivity towards the nitrile than the gas phase reaction. They also stated that the gaseous phase process is more adapted to short carbon chains (C ≤ 12) due their lower boiling point/lower reaction temperatures in compared to longer carbon chains (C ≥ 12) and that the liquid phase is more suitable for longer carbon chains than shorter carbon chains. They claimed that this is due the fact that higher reaction temperatures will cause more side reactions thus lowering the selectivity even more in a gas phase reaction. Therefore, only the liquid phase reactions will be studied.

2.2. Kinetic parameters

In this subchapter, the reaction mechanisms to produce nitriles will be described as well as the methods used to estimate several kinetic and thermodynamic parameters.

Reaction rate constant and reaction order

To understand more about the kinetics of these reactions, several kinetic parameters are looked into. The first kinetic parameters that are investigated are the reaction rate constants and the orders of the reactions which can be found in equation 3-6. In these equations the rate constants are denoted as k_1 , k_{-1} , k_2 and k_{-2} and the order as x , y , and z . These constants will be determined numerically with the help of experimental data. From the paper of Mekki-Berrada^[1], the reaction orders of acid, amide and nitrile are claimed to be of first order. This assumption will also be used in the calculations of the other kinetic parameters.

$$r_1 = k_1 \cdot [Acid] \cdot [NH_3]^x \quad [3]$$

$$r_{-1} = k_{-1} \cdot [Amide] \cdot [H_2O]^y \quad [4]$$

$$r_2 = k_2 \cdot [Amide] \quad [5]$$

$$r_{-2} = k_{-2} \cdot [Nitrile] \cdot [H_2O]^z \quad [6]$$

Arrhenius equation

The influence of temperature on the rates of chemical reactions is most commonly interpreted using the Arrhenius equation, which is shown in equation 7.^[6-8] This equation can be used to determine two important kinetic parameters, the activation energy and the pre-exponential factor.

The activation energy (E_A) represents the energy difference between reactants and an activated species. This activated species can be seen as an intermediate structure between reactants and products, such as a tautomer. Therefore, the activation energy is the minimum energy difference between reactant and their transitional state, and can often be specified as the height of the energy barrier opposing the reaction.^[7,8]

The pre-exponential factor (A) was originally a constant that came from integration but it was later suggested that the rate of reaction is a function of the number of activated molecules and their frequency of collisions. Therefore, this factor can often be seen as the number of true collisions multiplied with a probability factor.^[7,8]

In equation 8, a more simplistic linear equation is shown of the Arrhenius equation which is obtained by taking the natural logarithm over the equation. From this, an Arrhenius plot can be drawn which is shown in figure 1. The activation energy can be determined from the slope and the pre-exponential factor from the intersect-point with the y-axis. By determining these parameters, estimations can be made of the reaction rates at different temperatures.

$$k = A \cdot e^{\frac{-E_a}{R \cdot T}} \quad [7]$$

$$\ln(k) = \frac{-E_a}{R} \cdot \frac{1}{T} + \ln(A) \quad [8]$$

Van 't Hoff equation

The Van 't Hoff equation is widely used to obtain information of the changes in state functions in thermodynamic systems.^[10] The equation originated from the thermodynamic definition of the chemical equilibrium and from the equation of the standard Gibbs energy of reaction, which can be found in equation 9 and 10, respectively.^[8,11] Combining these equations will yield the nonlinear form of the Van 't Hoff equation (equation 11). Rearranging this equation, a well-known linear form of the Van 't Hoff equation is obtained as shown in equation 12.

These equations can be used to determine reaction enthalpy and entropy of the reaction. The enthalpy will give insight on the amount of heat that is needed or produced by the reaction. A negative enthalpy shows an exothermic reaction and a positive enthalpy will show an endothermic reaction. The entropy will give insight on the disorder of the system at which a positive entropy increased the disorder and vice versa.^[8,10]

The linear form of the Van 't Hoff equation can be used to determine the enthalpy and entropy graphically and an illustration of such plot is shown in figure 2. This plot relates the change in equilibrium constant of a chemical reaction to the change in temperature at the standard enthalpy and entropy change. From this plot, the enthalpy can be determined from the slope of the graph and the entropy can be found from the intersect-point with the y-axis.

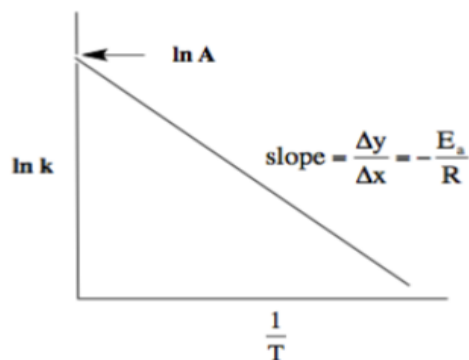


Figure 1: General illustration of the Arrhenius plot at which the activation energy and pre-exponential factor can be determined from the slope and y-axis intersection, respectively.^[9]

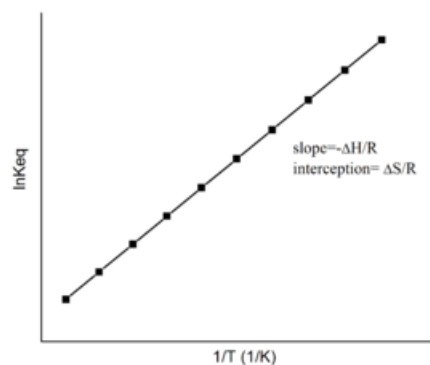


Figure 2: General illustration of the Van 't Hoff plot of an exothermic reaction at which the enthalpy and entropy can be determined from the slope and y-axis intersection, respectively.^[12]

$$\Delta_r G^\ominus = -R \cdot T \cdot \ln(K_{eq}) \quad [9]$$

$$\Delta_r G^\ominus = \Delta_r H^\ominus - T \cdot \Delta_r S^\ominus \quad [10]$$

$$-R \cdot T \cdot \ln(K_{eq}) = \Delta_r H^\ominus - T \cdot \Delta_r S^\ominus \quad [14]$$

$$\ln(K_{eq}) = \frac{-\Delta_r H^\ominus}{R} \cdot \frac{1}{T} + \frac{\Delta_r S^\ominus}{R} \quad [16]$$

2.2. Operational systems

In the following subchapter, the basic principles of operational systems that are used during this thesis are explained, the batch and continuous system.

Open batch system

Batch reactors are widely used in the chemical industry and are often employed in small-scale operation for testing new processes that not have been fully developed.^[13] In these type of reactors, the reaction material is added at the beginning of the reaction and no inflow nor outflow of material will occur during the reaction.^[13,14] The type of batch system that will be used during this thesis is an open batch system in which there is no inflow of reactant but gaseous compounds that are produced during the reactor, e.g. water and ammonia, are allowed to leave the system with the help of a continuous stream of nitrogen gas. This allows the system to stay at ambient pressure and allows for the removal of the harmful ammonia vapours that are produced during the reaction. There are also several disadvantages to this system, such as the time needed to heat the system to the desired reaction temperature but also the unknown water and ammonia concentrations in the liquid phase due to the constant evaporation/removal.

This setup can provide information about the concentration profiles over certain reaction times which can later be used to estimate the reaction orders and rate constants. Furthermore, the thermodynamic parameters cannot be determined in this setup because the systems is open and never reaches thermodynamic equilibrium.

Plug flow reactor

The continuous system that will be studied during this thesis is the plug flow reactor (PFR). This reactor has a continuous inflow and outflow of material. They often have a high area-to-volume ratio and therefore have a better heat/mass transfer and require less development to upscale than traditional batch reactors.^[13] As for the kinetics, a PFR behaves similar as a batch reactor due the fact that the volume travels through the reactor as a plug.^[14,15] Under the assumption that there is no back mixing, this plug can be seen as its own small batch reactor that will react over time corresponding to the residence time. Therefore, the plug flow reactor is ideal for a comparison with the batch system.

The continuous setup will also provide information about the concentration profiles over several residence times which can be used to estimate the reaction orders and rate constants. Furthermore, at high residence times an equilibrium will be reached which can be used to determine the equilibrium constant. With this equilibrium constant, an estimation can be made over the enthalpy and entropy of the reactions.

2.3. Gas chromatography

Gas chromatography (GC) is widely used in analytical chemistry for separating and analysing compounds that can be vaporized without decomposition.^[16] A diagram of a gas chromatograph can be found in figure 3.

The GC can separate the compounds by injecting the sample in a mobile phase, typically called the carrier gas, and pass it through a stationary phase. The mobile

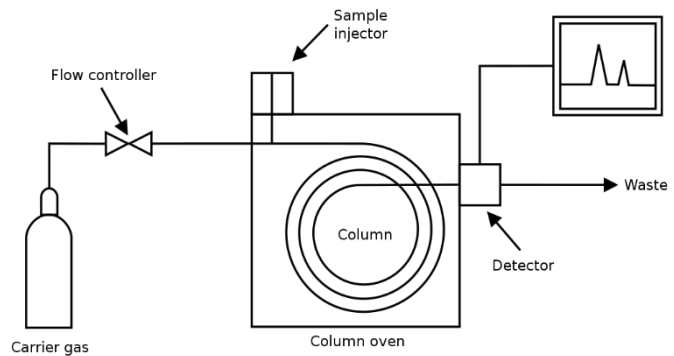


Figure 3: Diagram of a gas chromatograph^[17]

phase is usually an inert gas or an unreactive gas to the compounds. The stationary phase is a microscopic layer of viscous liquid which is either applied directly on the inner walls of the GC-column or on solid particles which reside in the column. As the carrier gas transports the sample through the column, adsorption is taking place between the molecules and the stationary phase. Since each compound has a different affinity toward the stationary phase, a separation is taking place throughout the column at which each compound reaches the detector at different retention times. The detector, commonly a flame ionization detector (FID), is used to monitor the time at which each component reaches the outlet and the intensity of it which can later on be linked to the amount of component using a calibration line of that component.

3. Experimental

3.1. Materials

The materials and the equipment needed for this project are summarised in table 1 and 2.

Table 1: Materials

Name	Type	Supplier	Additional information
Oleic amide	301-02-0	TCI-Chemicals	Lot. WDTRI-NR; 85 wt% purity
Oleic acid	112-80-1	VWR Chemicals	Lot. 19K084004; 79 wt% purity
Oleic nitrile	112-91-4	Nouryon	Lot. 2041060; 77 wt% purity
Lauric amide	1120-16-7	TCI-Chemicals	Lot. ZK57I-ML; 96% wt% purity
Lauric acid	143-07-7	TCI-Chemicals	Lot. GZFOD-GG; 98% wt% purity
Lauric nitrile	2437-25-4	TCI-Chemicals	Lot. FGN01COHJ; 98% wt% purity
Isopropanol	67-63-0	VWR Chemicals	Lot. 20F124015; 98% wt% purity

Table 2: Equipment

Name	Type	Supplier	Additional information
Batch setup	[-]	[-]	Consists of different pieces of glass work, heating mantle with magnetic stirrer, and supply of nitrogen gas.
Flow setup	[-]	[-]	Consists of multiple stainless steel Swagelok parts, Dockweiler tubing, heating coil, and temperature controllers.
Gas chromatograph	GC-2010 Plus	Shimadzu	With an FID detector and auto sampler

3.2. Method

The methods used during this project can be subdivided in three major topics: the batch setup, the continuous setup and the modelling using Matlab. In the following sub-chapters, each of these methods are introduced separately.

Batch setup

The batch setup is used to convert oleic amide to oleic nitrile and oleic acid. The setup behaves as an open batch system and a schematic is shown in figure 4.

In this setup, the oleic amide is heated by a heating plate (2) to the desired temperature. The reaction takes place in the reaction flask (1) in which water and ammonia is constantly purged out of the system into an ammonia-water trap (5) using nitrogen as purge gas. This continuous purge causes an ammonia and water poor environment. Furthermore, a condenser (3) is added to ensure no oleic compounds are leaving the system and a small collection flask (4) is installed to collect any condensate along the walls.

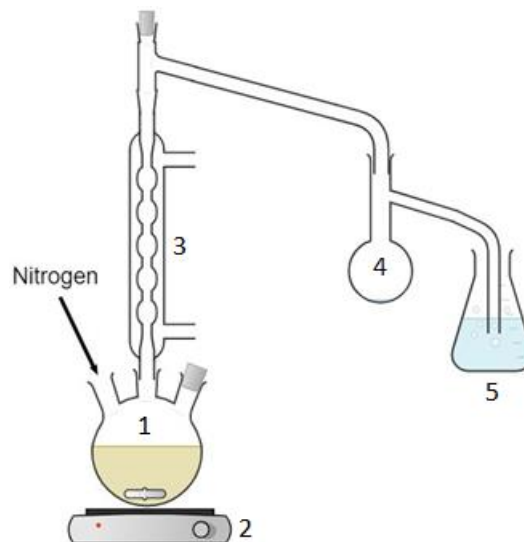


Figure 4: Schematic of the batch setup. (1) Reaction flask. (2) Heating plate. (3) Condenser. (4) Water collection flask. (5) Ammonia-water trap.

The reaction temperatures that were investigated are 270, 300 and 330 °C. But due the fact that the 30 grams of reaction mixture have to be heated from room temperature, a temperature gradient will be highly likely to be seen over time at the start of the reaction. The heat-up time is minimized by pre-heating and well isolating the setup. The samples will be taking directly out of the reaction flask using glass pipettes at certain time intervals.

Approximately 100 mg of each these samples were weighed and then dissolved using 1 ml of isopropanol. The samples will then be analysed using gas chromatography. A calibration line for each of the compounds was used to determine the mass of the compounds in the sample. From the mass, a concentration can be calculated using the molar weight and density (under the assumption of a constant density of 883 kg/m³).

Continuous system

The continuous operation is used to convert oleic amide to oleic nitrile and oleic acid. The setup is designed as a plug flow reactor and a schematic is shown in figure 5.

In this figure, the oleic amide is stored in a storage vessel (1) and is pushed through the system using nitrogen gas. This storage vessel is preheated to melt the amide and to lower the temperature gradient when it reaches the capillary reactor (3). When in the reactor, the amide is heated to the desired temperature using a heating coil and is flowing through the capillary in plug flow. A needle valve (4) is installed to adjust the flowrate through the system and a collection vessel (5) is added at the end of the reactor. Furthermore, several pressure and temperature indicators are installed to record the reaction conditions and the storage vessel is equipped with a safety valve (2) to ensure the system opens if there is a too high pressure build up.

The heated part in the capillary reactor is 2 m long and has an inner diameter of 2.054 mm which equals to a reactor volume of 6.63 ml.

The flowrate in the system has to be determined before taking a sample to estimate the time needed to purge and rest to reach a steady state. The flowrate was determined by weighing the mass flowing out of the system over a certain period of time while assuming a constant density in the reactor. The system was then allowed to further rest and come to a steady state until a total of 1.5x residence time has passed. After which, a sample of approximately 2.5x the reactor volume is taken to reduce experimental error and the sample mass, sampling time and reaction temperatures had been recorded.

For the analysis, the samples were reheated and mixed thoroughly. Approximately 100 mg of each these samples were weighed and then dissolved using 1 ml of isopropanol. The samples will then be analysed using gas chromatography. A calibration line for each of the compounds was used to estimate the mass of the compounds in the sample. From the mass, a concentration can be calculated using the molar weight and density (under the assumption of a constant density of 883 kg/m³).

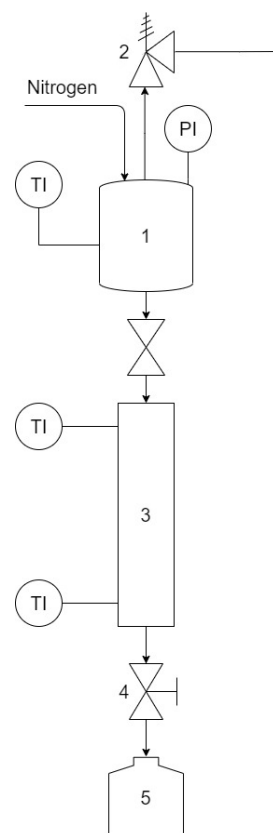


Figure 5: Schematic of the flow setup. (1) Storage vessel. (2) Safety valve. (3) Capillary reactor. (4) Needle valve. (5) Collection vessel.

Modelling

In order to estimate the reaction rate constants and order in the reactions, a system of differential equations must be solved, which can be found in equations 13-17. These equations are based on the reaction rate equation in equation 3-6.

This task is solved numerically employing Matlab to estimate the reaction rate constants and order using experimental data. This is done with the use of the built-in Matlab-function “ode15s” and “lsqnonlin”. The Matlab scripts can be found in appendix I.

The ode15s-function is used to solve a system of ordinary differential equations over the reaction time using initial guesses of the k-values and orders. The theoretical data from the ode-solver is then compared with the experimental data to calculate the error of the system. The error of the system is then fed to the lsqnonlin-function which adjusts the k-values or order in the reactions and runs the ode-solver again. This process is repeated until a minimum of errors is reached between the theoretical data and the experimental results.

The experimental data that is used for the estimation came from the flow setup and a few assumptions are made. One of which is that the density of the reaction mixture remains constant. The second assumption is that all the components stay in one homogenous phase.

$$\frac{d[\text{Nitrile}]}{dt} = (k_2 \cdot [\text{Amide}]) - (k_{-2} \cdot [\text{Nitrile}] \cdot [\text{H}_2\text{O}]^z) \quad [13]$$

$$\frac{d[\text{Acid}]}{dt} = (k_{-1} \cdot [\text{Amide}] \cdot [\text{H}_2\text{O}]^y) - (k_1 \cdot [\text{Acid}] \cdot [\text{NH}_3]^x) \quad [14]$$

$$\frac{d[\text{Amide}]}{dt} = (k_1 \cdot [\text{Acid}] \cdot [\text{NH}_3]^x) + (k_{-2} \cdot [\text{Nitrile}] \cdot [\text{H}_2\text{O}]^z) - (k_{-1} \cdot [\text{Amide}] \cdot [\text{H}_2\text{O}]^y) - (k_2 \cdot [\text{Amide}]) \quad [15]$$

$$\frac{d[\text{H}_2\text{O}]}{dt} = (k_{-1} \cdot [\text{Amide}] \cdot [\text{H}_2\text{O}]^y) + (k_2 \cdot [\text{Amide}]) - (k_1 \cdot [\text{Acid}] \cdot [\text{NH}_3]^x) - (k_{-2} \cdot [\text{Nitrile}] \cdot [\text{H}_2\text{O}]^z) \quad [16]$$

$$\frac{d[\text{NH}_3]}{dt} = (k_{-1} \cdot [\text{Amide}] \cdot [\text{H}_2\text{O}]^y) - (k_1 \cdot [\text{Acid}] \cdot [\text{NH}_3]^x) \quad [17]$$

4. Results

In this chapter, the results of the most important experiments are listed. This includes the results of the batch system, mass losses, flow system, Arrhenius constants, and Van 't Hoff constants.

4.1. Batch system

During this project, several experiments are done in batch operations. The concentration profiles at this temperature of the different oleic compounds are shown in figure 6. From this figure, several conclusions can be drawn. First of which is a plateau during the first 20 minutes of reaction at which the concentrations change insignificantly. This is due to the temperature gradient caused by heating up the reaction mixture to the reaction temperature. From the temperature graph in figure 6, the concentrations change insignificantly until the reaction reaches around 250 °C.

Another notable observation is that the all the amide in the system was converted. This is due the fact that the batch system is an open system which allows for a continuous purge of ammonia and water out of the system and thus changing the equilibrium state to deplete the amide.

At last, the reactions toward acid continues to increase over the time (up to 100 min) even though gaseous water is continuously purged out of the system, meaning that there is still a significant amount of water present in the liquid phase at 300 °C. This result could provide evidence that water has a mass transfer limitation in the liquid phase even at these temperatures.

At 300 °C, the amide reached a 90 % conversion after 90 minutes with a nitrile and acid yield of 60 % and 27 %, respectively.

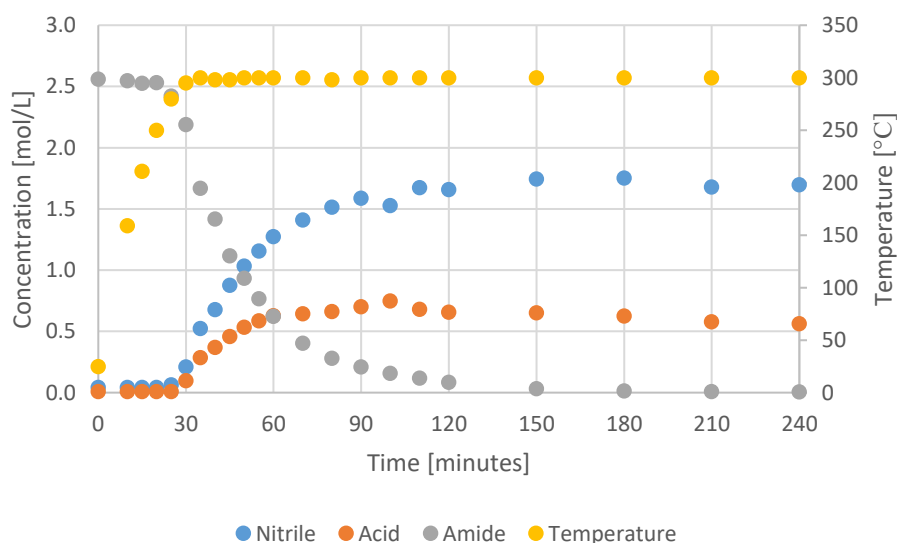


Figure 6: Concentration profiles of oleic nitrile, acid and amide (left-axis) and temperature profile (right-axis) at 300 °C in the batch setup

Additionally, different temperatures have been investigated to show the effects of temperature on the reaction in the batch system. The results of 270 and 330 °C can be seen in figure 7 and 8. The graphs show that at lower temperatures, the reactions are slower. This is expected, just as the reaction proceeding faster at higher temperatures.

At 270 °C, the amide reached a 90 % conversion at 240 minutes with a nitrile and acid yield of 49 % and 23 %, respectively. And at 330 °C, the amide reached a 90 % conversion at 70 minutes with a nitrile and acid yield of 48 % and 18 %, respectively.

Furthermore, the graphs at reaction temperature of 330°C show a decline in the acid and nitrile concentrations at later reaction times: the mass of oleic compounds in the system is decreasing. This phenomenon will be further investigated in the next chapter.

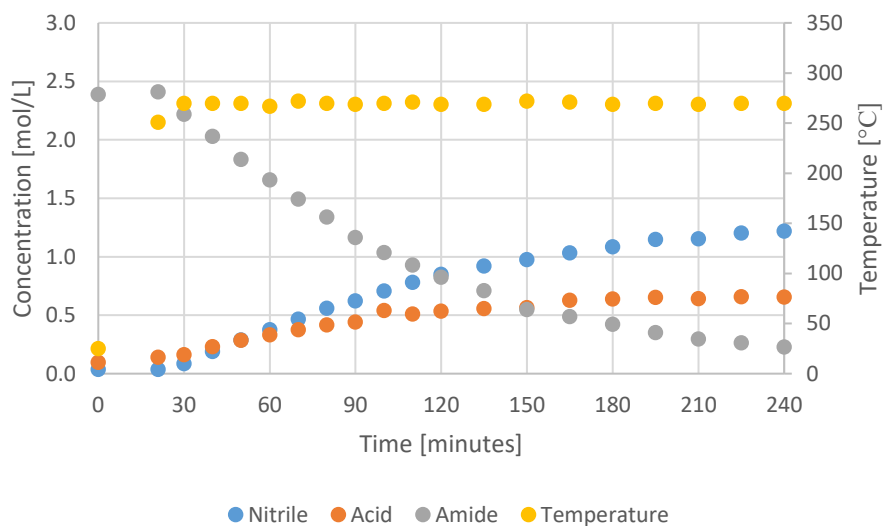


Figure 7: Concentration profiles of oleic nitrile, acid and amide (left-axis) and temperature profile (right-axis) at 270 °C in the batch setup

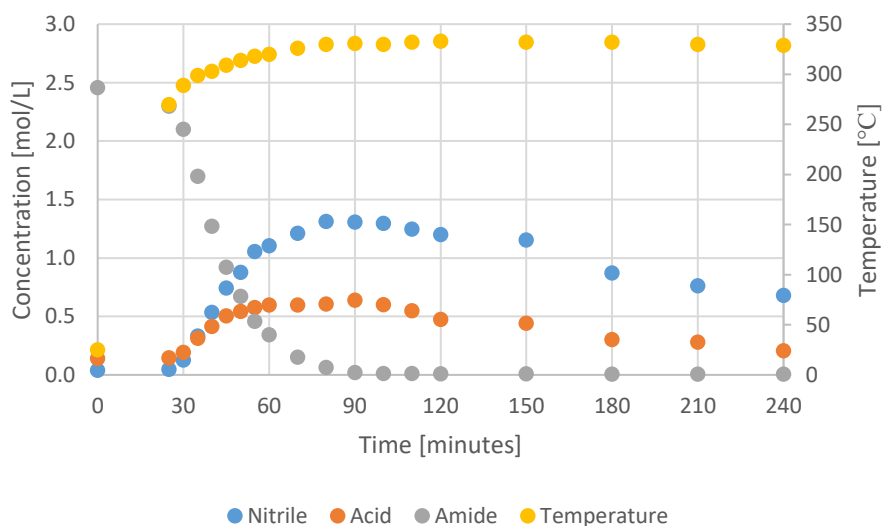


Figure 8: Concentration profile of oleic compounds at 330 °C in the batch setup

4.2. Investigation of product losses in oleic compounds

As previously mentioned, product losses of the oleic compounds occur over the course of the reaction. In figure 9, the losses of oleic compounds at different reaction temperatures are compared over time. Even at temperatures of 270 and 300 °C, a loss of around 15 % occurs and a significant 65 % of loss is seen at 330 °C. It is hypothesized that this phenomenon can either be caused by mass loss of these components by evaporating out of the system or a side reaction of the oleic components.

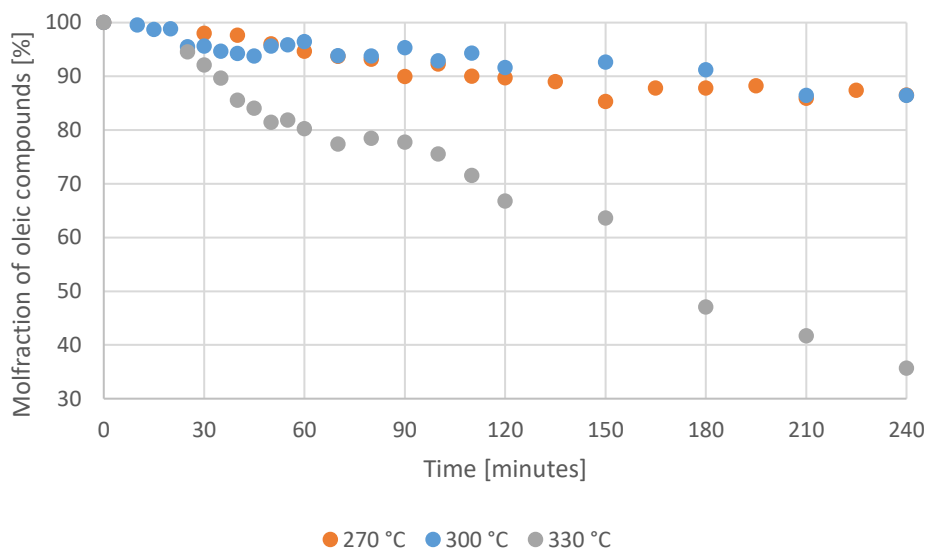


Figure 9: Loss of oleic compounds at different reaction temperatures

Studying the evaporation rates of oleic compounds

Evaporation could be a logical explanation for the mass losses since the reaction temperatures are relatively close to the boiling points of oleic acid and oleic nitrile, 360 and 386 °C respectively. Prior to the current batch setup, no condenser was added which could have led to evaporation of oleic compounds out of the system.

To check this hypothesis, a condenser was added and experiments of 300 °C were repeated with the addition of a condenser and compared with the results of a reaction without condenser as seen in figure 10. Between these graphs, no significant changes can be seen between the results with and without condenser. Plus, the mass before and after the experiment with the condenser were measured: From the original 30 grams of starting reactant, only 0.9 grams have left the system. From the amount of moles of oleic acid and nitrile that was produced, this mass loss is high likely the water (0.5 gram) and ammonia (0.4 gram) vapour. Therefore, evaporation is not the cause of the observed mass loss.

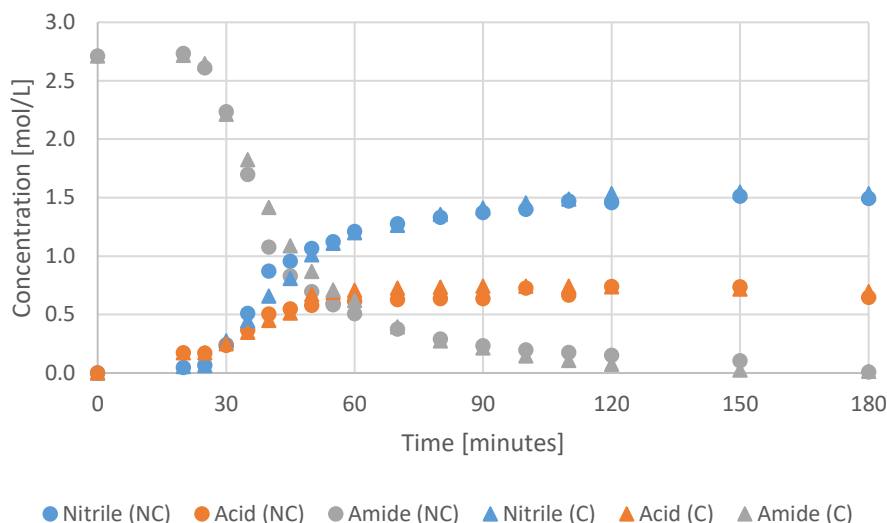


Figure 10: Effect on the concentration profiles with condenser (C) and without condenser (NC)

Studying the possibilities of side reactions

Certain side reactions with the oleic compounds could lead to unseen mass losses especially if these compounds cannot be identified during the analysis. The purity of the starting reactant, oleic amide, is around 85 wt%. The other 15 % consist amides and nitriles of different carbon chain lengths (a qualitative GS-MS analysis is added in appendix X). To test if these impurities have an influence, 96 wt% pure lauric amide was used as starting reactant which has a similar chemical structure as oleic amide. Lauric amide has a shorter carbon chain (C_{12} -chain) and is fully saturated, unlike oleic amide which has C_{18} -chain and a double bond.

The results with lauric amide are shown in figure 11. In this experiment, the reaction with lauric amide was done at different stages of temperature, starting from 250 °C and going up to 284 °C at which the boiling point was reached of lauric nitrile. During this period, no significant losses between the lauric compounds can be seen.

At the end of the experiment, a weak acid was added to the system in the form of a few droplets of oleic acid. After the addition of oleic acid, a sudden loss in lauric compounds is observed. The cause of this behaviour is likely the addition of an unsaturated bond in the hydrocarbon chain. The reason for this hypothesis is the fact that carboxyl-groups were already present in the form of lauric acid prior to the addition of oleic acid and no significant losses have been observed during this period. The only difference between these two compounds is the unsaturated bond of oleic acid which could lead to polymerization of the hydrocarbon chains. These long chain hydrocarbons molecules would then be unable to vaporize in the gas chromatograph and be filtered out during the analysis of the samples. But further research has to be done to confirm the possibilities of radical polymerization between these compounds at these temperatures.

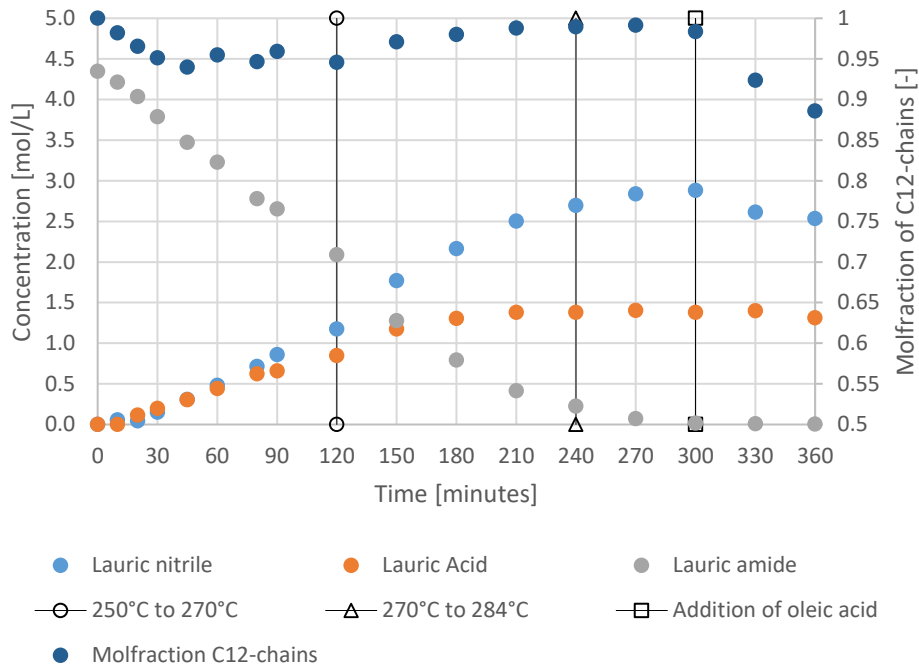


Figure 11: Concentration profile of lauric compounds at different temperature ranges

4.3. Continuous system

During this project, a continuous plug flow reactor was constructed. Similar experiments were done on the flow system as like in the batch system, the reaction of oleic amide at different temperatures. These experimental results are also used to estimate k-values and order in the different reactions (see equation 3-6) and to model the reactions using Matlab.

The concentration profile of the flow setup at 300 °C is shown in figure 12. Because the system is closed, the reaction mixture can reach an equilibrium state. This equilibrium is reached at around 25 minutes of residence time and only a 55 % amide conversion is reached with a nitrile and acid yield of 29 % and 21 %, respectively.

When not taking in to account the temperature delay, the batch system is able to obtain a similar conversion (56 %) at around 25 minutes of reaction time with a nitrile and acid yield of 32 % and 18 %, respectively. The results between these two experiments are similar, which was expected between a plug flow reactor and batch reactor. Despite this, the batch system does perform slightly better in terms of yield. This could either be experimental error or the fact that there is a continuous purge of ammonia and water which favours the reaction of nitrile over acid.

Also, a theoretical model has been constructed from the k-value and order estimations in Matlab. The model and experimental data seem to be in line with each other. The values of the reaction rate constants and reaction orders at 300 °C are estimated to be:

- $k_1 = 23.11 \text{ ml}^x / (\text{mol}^x \cdot \text{min})$ with, $x = 0.75$
- $k_{-1} = 44.29 \text{ ml}^y / (\text{mol}^y \cdot \text{min})$ $y = 0.75$
- $k_2 = 3.795 \cdot 10^{-2} / \text{min}$ $z = 0.92$
- $k_{-2} = 156.38 \text{ ml}^z / (\text{mol}^z \cdot \text{min})$

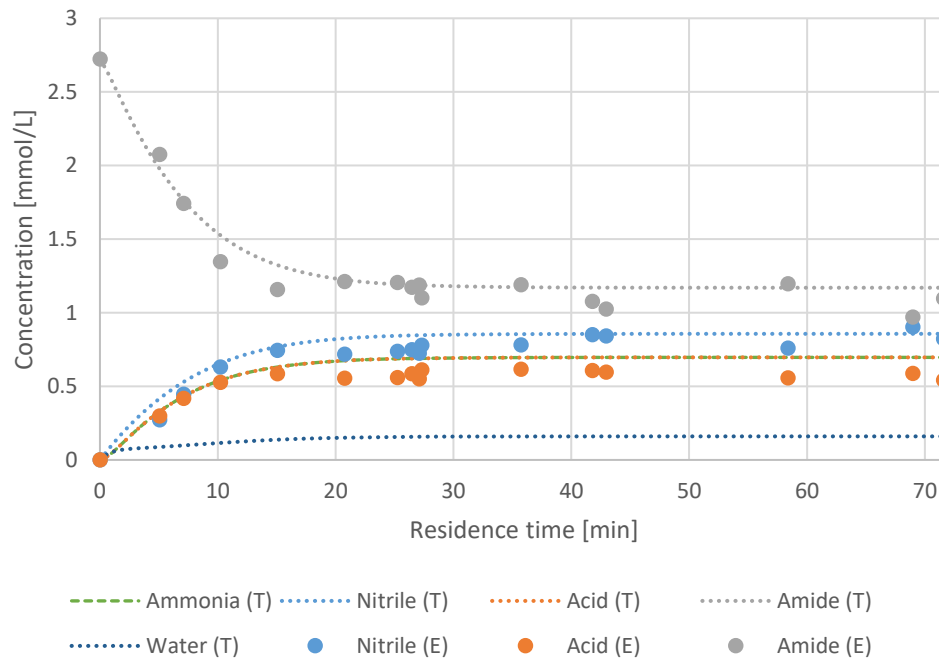


Figure 12: Concentration profile of oleic compounds at 300 °C in the flow setup at which the theoretical model is denoted as (T) and the experimental data as (E).

Furthermore, different temperatures have been investigated to show the effect of reaction temperature in the flow system. The results from 270 and 250 °C can be seen in figure 13 and 14. The behaviour of the reaction at these lower temperatures is consistent with the one seen at 300 °C; an equilibrium is reached after a set amount of time. Also, the values of the reaction orders have been kept the same as of the 300 °C experiment.

This equilibrium at 270 °C is reached at around 12 minutes of residence time and a 38 % amide conversion is observed with a nitrile and acid yield of 17 % and 14 %, respectively. The values of the reaction rate constants and reaction orders at 270 °C are calculated to be:

- $k_1 = 114.55 \text{ ml}^x / (\text{mol}^x \cdot \text{min})$ with, $x = 0.75$
- $k_{-1} = 152.53 \text{ ml}^y / (\text{mol}^y \cdot \text{min})$ $y = 0.75$
- $k_2 = 3.121 \cdot 10^{-2} / \text{min}$ $z = 0.92$
- $k_{-2} = 855.22 \text{ ml}^z / (\text{mol}^z \cdot \text{min})$

This equilibrium at 250 °C is reached at around 10 minutes of residence time and a 22 % amide conversion is observed with a nitrile and acid yield of 10 % and 10 %, respectively. The values of the reaction rate constants and reaction orders at 270 °C are calculated to be:

- $k_1 = 263.47 \text{ ml}^x / (\text{mol}^x \cdot \text{min})$ with, $x = 0.75$
- $k_{-1} = 280.17 \text{ ml}^y / (\text{mol}^y \cdot \text{min})$ $y = 0.75$
- $k_2 = 1.914 \cdot 10^{-2} / \text{min}$ $z = 0.92$
- $k_{-2} = 1967.00 \text{ ml}^z / (\text{mol}^z \cdot \text{min})$

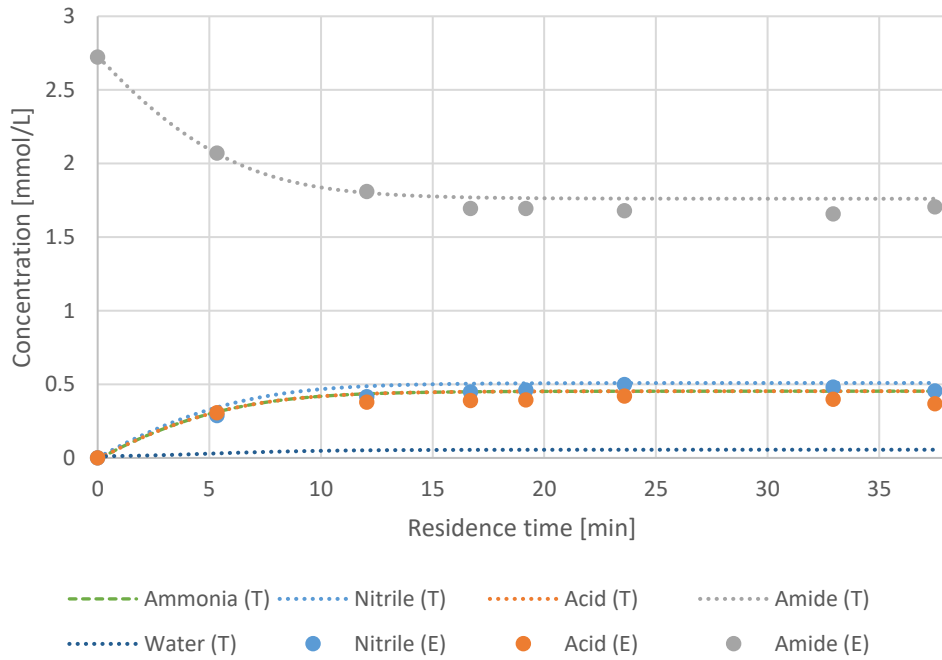


Figure 13: Concentration profile of oleic compounds at 270 °C in the flow setup at which the theoretical data is denoted as (T) and the experimental data as (E).

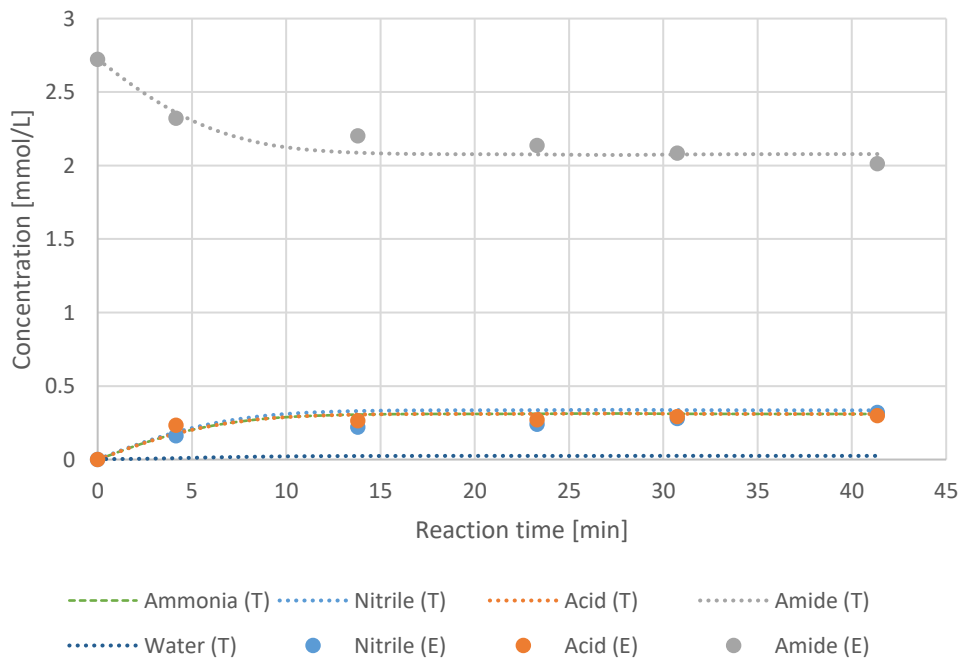


Figure 14: Concentration profile of oleic compounds at 250 °C in the flow setup at which the theoretical data is denoted as (T) and the experimental data as (E).

4.4. Arrhenius plot

An Arrhenius plot is used to obtain the activation energy and pre-exponential constant of the reactions using the results from the flow setup and the estimation of the rate constants. The results of the plot can be found in table 3 and figure 15. A noticeable remark is the fact that certain activation energies are negative which is most unlikely in these reactions. Also, certain rate constants appear to have a higher rate a lower temperatures which is quite counter intuitive. It high likely that the estimation of the k-values are incorrect, even though the modelled data fit quite well with the experimental data.

One possible explanation for incorrect k-values, could be the cause of one of the assumptions that were made to estimate the k-values. The assumption that is made is that all the components in the plug flow reactor would stay in one homogenous phase. This is incorrect for water and ammonia at these high temperatures. Attempts have been made to model these compounds in a gas-phase and using Henry coefficients or saturation pressures to calculate the liquid but resulted in unrealistic models such as negative concentration and non-equilibrium behaviour.

Table 3: Results of the Arrhenius plot

Temperature		k_1	k_{-1}	k_2	k_{-2}
[°C]		[ml ² /(mol ² ·min)]	[ml ³ /(mol ³ ·min)]	[1/min]	[ml ² /(mol ² ·min)]
250		263.47	280.17	0.01914	1967.00
270		114.55	152.53	0.03121	855.22
300		23.11	44.29	0.03795	156.38
Slope	[-]	14706	11161	-3979	15321
Y-intersection	[-]	-22.47	-15.64	3.729	-22.62
R²	[-]	0.9918	0.9891	0.8934	0.9890
Activation energy	[J/mol]	-122266	-92793	33085	-127379
Pre-exponential constant	[-]	$1.743 \cdot 10^{-10}$	$1.613 \cdot 10^{-7}$	41.65	$4.075 \cdot 10^{-10}$

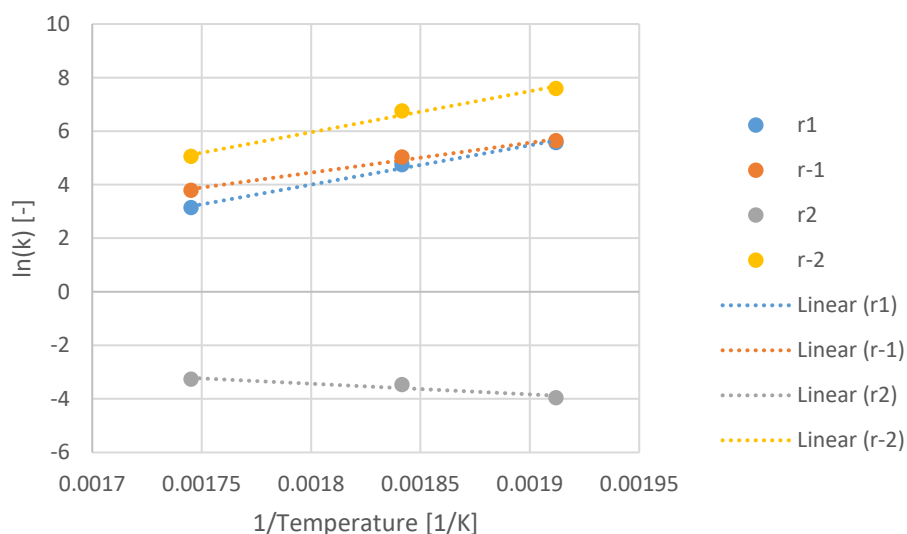


Figure 15: Arrhenius plot of the different reactions

4.5. Van 't Hoff plot

The Van 't Hoff plot is used to obtain the enthalpy and entropy of the reactions using the results from the flow setup at equilibrium at different temperatures. In table 4 and figure 16, the results of the Van 't Hoff plot is shown at which the correlation between the equilibrium constants and temperature show a good linear fit.

The first reaction from oleic acid toward oleic amide has a negative enthalpy which means that this reaction is exothermic. This reaction also has a negative entropy, meaning that the disorder decreases when going from reactants to products.

For the second reaction from oleic amide toward oleic nitrile, the enthalpy is positive which means that this reaction is endothermic. This reaction also has a positive entropy, meaning that the disorder increases when going from reactants to products.

When comparing the two enthalpies, the enthalpy of the second reaction is far greater than that of the first reaction, nearly 10 times higher, thus the overall reaction from oleic acid toward oleic nitrile is endothermic. The overall heat required to convert acid into nitrile equals to 151 kJ/mol which is of the same order of magnitude as what Shirazi et al. (2017) found which was 271 kJ/mol.

Table 4: Results of the Van 't Hoff plot

Temperature		$K_{eq, reaction_1}$	$K_{eq, reaction_2}$
[°C]		[-]	[-]
250		0.5401	0.0040
270		0.4772	0.0161
300		0.3855	0.1171
Slope	[-]	2031	-20234
Y-intersection	[-]	4.494	33.158
R²	[-]	0.9961	0.9999
Enthalpy	[J/mol]	-16892	168225
Entropy	[J/K]	-37.36	275.68

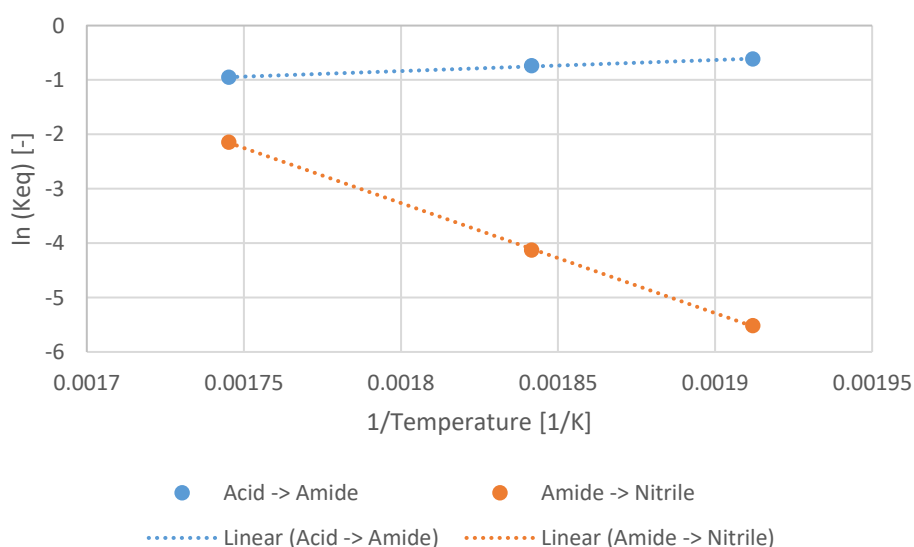


Figure 16: Van 't Hoff plot of the reactions

5. Conclusion and recommendations

5.1. Conclusion

During the course of this thesis, kinetic studies have been carried out on the reaction mechanisms of oleic amide into oleic nitrile and oleic acid in batch and flow systems during which a fully working plug flow reactor was build.

Batch operation

Using the batch system, several experiments were carried out at different temperatures, 270, 300 and 330 °C. The experiment at 270 °C shows an amide conversion of 90 % after 240 minutes with a nitrile and acid yield of 49 % and 23 %, respectively. At 300 °C, an amide conversion of 90 % is reached after 90 minutes with a nitrile and acid yield of 60 % and 27 %, respectively. And at last, the reaction at 330 °C shows a conversion of 90 % after 70 minutes with a nitrile and acid yield of 48 % and 18 %, respectively.

As expected, the reactions of amide is faster at higher temperatures, but the product yields seem to be depended on the amount of side reactions occurring during the time of reaction. Especially at higher temperatures where side reaction start to occur more often even at low reaction times, high product losses are seen and therefore lowers the nitrile yields.

Furthermore, the reaction toward the acid continues to happen over time, even though there is a continuous purge of water in the gas phase. This could provide evidence that water has a mass transfer limitation in the liquid phase even at 300 °C.

From the experiment with lauric amide, it can be seen that the cause of these side reactions are likely due to reactions with the unsaturated bonds in the carbon chains. It is hypothesized that these bonds undergo a polymerization reaction but further investigation is needed to support this hypothesis.

Continuous operation

The reaction rate constants and orders have been estimated using Matlab at 250, 270 and 300 °C. The order of x, y, and z are estimated to be 0.75, 0.75 and 0.92, respectively. The rate constants at 250, 270 and 300 °C are as followed:

- k_1 : 263.47, 114.55 and 23.11 ml^x/(mol^x·min), respectively;
- k_{-1} : 280.17, 152.53 and 44.29 ml^y/(mol^y·min), respectively;
- k_2 : $1.914 \cdot 10^{-2}$, $3.121 \cdot 10^{-2}$ and $3.795 \cdot 10^{-2}$ min⁻¹, respectively;
- k_{-2} : 1967, 855.22 and 156.38 ml^z/(mol^z·min), respectively.

Furthermore, the experimental data closely resemble the theoretical model at each reaction temperature. The experiments at 250 °C shows an equilibrium at 10 minutes with an amide conversion of 22 % along with a nitrile and acid yield of 10 %. At 270 °C, an equilibrium is reached at 12 minutes with a conversion of 38% together with a nitrile and acid yield of 17 % and 14 %, respectively. At last, the 300 °C experiments show an equilibrium state at 25 minutes with a conversion of 55 % along with a nitrile and acid yield of 29 % and 21 %.

When comparing the batch and continuous operations at 300 °C, the batch system is able to achieve similar results as the continuous operations at 25 minutes of reaction time after which an equilibrium is reached in the PFR. The conversion of amide in the batch is able to proceed further due to the continuous purge of water and ammonia thus leading to higher conversions and higher nitrile yields. Therefore, the batch system performed better than the continuous system.

Arrhenius plot

The activation energy and pre-exponential constant were calculated from an Arrhenius plot. The results show negative energies for the activation energy for 3 of the 4 reactions which is not possible for these reactions. It is hypothesized that this is likely due to a wrong assumption that all components will fully remain in one homogenous phase in the PFR which is incorrect for water and ammonia at high temperatures. Attempts have been made to re-adjust the model using Henry coefficients or saturation pressures but resulted in unrealistic models. Further research has to be done on this subject to develop a more realistic model.

Van 't Hoff plot

The enthalpy and entropy of the reactions were calculated from a Van 't Hoff plot. From this, it is shown that the reaction from oleic acid to oleic amide is slightly exothermic with an enthalpy of - 16.9 kJ/mol and increases the overall disorder in the system with an entropy of -37.36 J/K. In contrast, the reaction from oleic amide to oleic nitrile is highly endothermic with an enthalpy of 168 kJ/mol and decreases the overall disorder in the system with an entropy of 275.68 J/mol.

5.2. Recommendations

In this subchapter, several recommendations are discussed to improve either the analysis, model or the operational systems.

Further investigations on the possible side reactions

As previously mentioned, side reactions are likely to happen with the unsaturated bonds in the carbon chains thus lowering the overall nitrile yield. It is hypothesized that polymerization reaction could occur at these unsaturated bonds which increase the size of the molecule, thus being unable to be vaporized by GC and not characterised. Therefore, a new characterization method is needed to support the hypothesis.

An interesting method to look at would be size-exclusion chromatography at which a solution is separated by their size/molecular weight. This principle works by trapping smaller molecules in the pores of the adsorbent (stationary phase) thus allowing larger molecules to elute faster.^[18,19] Therefore, size-exclusion chromatography could be used to analysis the reaction mixture for higher molecular weight molecules.

Modelling the gas phase and liquid phase

Water and ammonia are currently modelled in one homogeneous phase with the other components. Attempts have been made to model the water and ammonia in the gas phase using correlations with Henry coefficients or saturation pressures to determine the concentration of water and ammonia in the liquid phase. These attempts resulted in unrealistic models and further studies have to be done on this subject.

Improving the PFR with better flow control

Currently, the plug flow reactor is fully operational but not optimal. One of the main issues in the design of the PFR is that there is no method to set the flow to a certain flowrate. It currently uses a needle valve which uses a spring mechanism to suppress the flow. Therefore, the flow is also dependent on the pressure and temperature in the system.

Due to the high melting point of oleic amide, around 80 °C, a conventional pump cannot be used. A better option is to use a heated extruder injection mechanism which allows flow control by adjusting the rotation speed of the extruder. The other benefit of this system is the improved solid handling and therefore excluding the need for the closed pre-heated storage vessel.

These extruders are already widely used in the polymer industry and have been studied and developed extensively, even to the extent that the pharmaceutical industry have started to use extruders as a dosing unit.^[20,21] Therefore, extruders would be an interesting topic to study to improve the plug flow reactor.

Changing the PFR into a packed bed reactor

By changing the flow reactor into a packed bed reactor, catalytic reactions can also be studied. This opens more research potential to improve the conversion, yield and selectivity of the reactions.

Furthermore, molecular sieves can be used in the packed bed reactor. These sieves act as a water adsorbent and can change the equilibrium of the reaction to benefit the production of nitriles.^[22,23] Initial experiments with molecular sieves in the batch reactor shown improved nitrile production. These results can be found in appendix III.

References

- (1) Mekki-Berrada, A.; Bennici, S.; Gillet, J. P.; Couturier, J. L.; Dubois, J. L.; Auroux, A. Ammoniation-Dehydration of Fatty Acids into Nitriles: Heterogeneous or Homogeneous Catalysis? *ChemSusChem* **2013**, *6* (8), 1478–1489. <https://doi.org/10.1002/cssc.201300210>.
- (2) Shirazi, Y.; Tafazolian, H.; Viamajala, S.; Varanasi, S.; Song, Z.; Heben, M. J. High-Yield Production of Fatty Nitriles by One-Step Vapor-Phase Thermocatalysis of Triglycerides. *ACS Omega* **2017**, *2* (12), 9013–9020. <https://doi.org/10.1021/acsomega.7b01502>.
- (3) DeVito, C. Nitriles. *Kirk-Othmer Encyclopedia of Chemical Technology* **2007**. <https://doi.org/10.1021/acsomega.7b01502>.
- (4) County, H. U.S. Patent 2993926. Method of Preparing Nitriles. **1957**, 3–6.
- (5) F. B. Bizhanov, E.Kh. Yazbaev, Zh. Prnazarov, *Izv. Akad. Nauk. Kaz. SSR, Ser. Khim.* **1985**, *4*, 23–26.
- (6) Laidler, K. J. The Development of the Arrhenius Equation. *J. Chem. Educ.* **1984**, *61* (6), 494–498. <https://doi.org/10.1021/ed061p494>.
- (7) Grime. Quarterly Reviews. *Notes Queries* **1863**, *s3-IV* (94), 316. <https://doi.org/10.1093/nq/s3-IV.94.316-a>.
- (8) Atkins, P. and de Paula, J. (2014) *Atkins' Physical Chemistry*. 10th Edition, Oxford University Press, Oxford.
- (9) Wikipedia, Arrhenius equation. https://en.wikipedia.org/wiki/Arrhenius_equation (Last accessed on July 11, 2021)
- (10) Lima, E. C.; Gomes, A. A.; Tran, H. N. Comparison of the Nonlinear and Linear Forms of the van't Hoff Equation for Calculation of Adsorption Thermodynamic Parameters (ΔS° and ΔH°). *J. Mol. Liq.* **2020**, *311*, 113315. <https://doi.org/10.1016/j.molliq.2020.113315>.
- (11) Lima, E. C.; Hosseini-Bandegharai, A.; Moreno-Piraján, J. C.; Anastopoulos, I. A Critical Review of the Estimation of the Thermodynamic Parameters on Adsorption Equilibria. Wrong Use of Equilibrium Constant in the Van't Hoof Equation for Calculation of Thermodynamic Parameters of Adsorption. *J. Mol. Liq.* **2019**, *273*, 425–434. <https://doi.org/10.1016/j.molliq.2018.10.048>.
- (12) Wikipedia, Van 't Hoff equation. https://en.wikipedia.org/wiki/Van_%27t_Hoff_equation (Last accessed on July 11, 2021)
- (13) Denbigh, K.G., Turner, J.C.R. (1984). *Chemical Reactor Theory: An Introduction*, 3rd ed. Cambridge university press, Cambridge.
- (14) Levenspiel, O. (1999) *Chemical Reaction Engineering*. 3th Edition, John Wiley & Sons, Hamilton.
- (15) Fogler, H.S. (2009). *Elements of chemical Reaction Engineering*. New Jersey.
- (16) Harvey, D. (2000). *Modern analytical chemistry*. McGraw-Hill, Boston.
- (17) Wikipedia, Gas chromatography. https://en.wikipedia.org/wiki/Gas_chromatography (Last accessed on July 11, 2021)

- (18) Barth, H. G.; Boyes, B. E. Size Exclusion Chromatography. *Anal. Chem.* **1990**, *62* (12), 268–303. <https://doi.org/10.1021/ac00211a020>.
- (19) Kostanski, L. K.; Keller, D. M.; Hamielec, A. E. Size-Exclusion Chromatography - A Review of Calibration Methodologies. *J. Biochem. Biophys. Methods* **2004**, *58* (2), 159–186. <https://doi.org/10.1016/j.jbbm.2003.10.001>.
- (20) Dhaval, M.; Sharma, S.; Dudhat, K.; Chavda, J. Twin-Screw Extruder in Pharmaceutical Industry: History, Working Principle, Applications, and Marketed Products: An In-Depth Review. *J. Pharm. Innov.* **2020**. <https://doi.org/10.1007/s12247-020-09520-7>.
- (21) Lindt, J. T. A Dynamic Melting Model for a Single-screw Extruder. *Polym. Eng. Sci.* **1976**, *16* (4), 284–291. <https://doi.org/10.1002/pen.760160411>.
- (22) Breck, D. W. ‘ Revolt T6e New England Association of Chem Chers. **1956**, *1956* (12).
- (23) Komarneni, S.; Pidugu, R.; Menon, V. C. Water Adsorption and Desorption Isotherms of Silica and Alumina Mesoporous Molecular Sieves. *J. Porous Mater.* **1996**, *3* (2), 99–106. <https://doi.org/10.1007/BF01186039>.

Appendix I: Matlab files

Main file: estimate_kinetic_parameters.m

```

%% Clear workspace
clc
clearvars
close all

%% Defining data and parameters
% Assigning concentration [mol/ml] and time [min] to arrays
Data_1 = readmatrix('Data_2.xlsx','Range','A3:K18');
p.nitrile = Data_1(:,7);
p.acid = Data_1(:,8);
p.amide = Data_1(:,9);
p.h2o = Data_1(:,10);
p.nh3 = Data_1(:,11);
time = Data_1(:,2);

% Defining additional parameters and initial conditions
p.T = 300+273; %[K]
p.P = 1.5*100000; %[Pascal]

y0 = [p.nitrile(1); p.acid(1); p.amide(1); p.h2o(1); p.nh3(1)]; %Initial
concentration conditions

p.order_1 = 1; % Order of acid, forward first reaction
p.order_2 = 1; % Order of amide, backward first reaction
p.order_3 = 1; % Order of amide, forward second reaction
p.order_4 = 1; % Order of nitrile, backward second reaction

% Defining initial guesses
k1_guess = 23.1117;
k1r_guess = 44.29;
k2_guess = 0.03783;
k2r_guess = 155.4700;

k_guess = [k1_guess; k1r_guess; k2_guess; k2r_guess];

order5_guess = 0.7450;
order6_guess = 0.7533;
order7_guess = 0.9165;

order_guess = [order5_guess; order6_guess; order7_guess];

% Define boundary conditions
lb_k = [0; 0; 0; 0;];
ub_k = [inf; inf; inf; inf;];
lb_o = [0; 0; 0;];
ub_o = [inf; inf; inf;];

```

```

%% Using LSQNONLIN to estimate kinetic parameters
% Launch lsqnonlin algorithm for k values
[k_guess,resnorm,residual] =
lsqnonlin(@fitcrit_k,k_guess,lb_k,ub_k,[],time,y0,p,order_guess);
k_guess
resnorm

% Launch lsqnonlin algorithm for order
[order_guess,resnorm,residual] =
lsqnonlin(@fitcrit_order,order_guess,lb_o,ub_o,[],time,y0,p,k_guess);
order_guess
resnorm

%% Graph
time_ode = linspace(0,time(end));
[t,y] = ode15s(@system_of_ode,time_ode,y0,[],k_guess,order_guess,p);

hold on
plot(t,y(:,1),'g--', t,y(:,2),'r--', t,y(:,3),'b--')
plot(time,p.nitrile,'o g', 'LineStyle', 'none')
plot(time,p.acid,'o r', 'LineStyle', 'none')
plot(time,p.amide,'o b', 'LineStyle', 'none')

legend('Nitrile (T)', 'Acid (T)', 'Amide (T)', 'Nitrile (E)', 'Acid (E)',
'Amide (E)');
xlabel('Time')
ylabel('Concentration')
hold off

```

Error function for k-value: fitcrit_k.m

```

function [error] = fitcrit_k(k_guess, time, y0,p,order_guess)
% Run ode solver
[t,y] = ode15s(@system_of_ode,time,y0,[],k_guess,order_guess,p);

% Calculate error between model data and experimental data
error_nitrile = sum(abs(p.nitrile - y(:,1)));
error_acid = sum(abs(p.acid - y(:,2)));
error_amide = sum(abs(p.amide - y(:,3)));
error_h2o = sum(abs(p.h2o - y(:,4)));
error_nh3 = sum(abs(p.nh3 - y(:,5)));

error = [error_acid; error_amide; error_nitrile; error_h2o;];
end

```


Error function for orders: fitcrit_order.m

```
function [error] = fitcrit_order(order_guess, time, y0,p,k_guess)
% Run ode solver
[t,y] = ode15s(@system_of_ode,time,y0,[],k_guess,order_guess,p);

% Calculate error between model data and experimental data
error_nitrile = sum(abs(p.nitrile - y(:,1)));
error_acid    = sum(abs(p.acid    - y(:,2)));
error_amide   = sum(abs(p.amide   - y(:,3)));
error_h2o     = sum(abs(p.h2o     - y(:,4)));
error_nh3     = sum(abs(p.nh3     - y(:,5)));

error = [error_acid; error_amide; error_nitrile];
end
```

ODE function: system_of_ode.m

```
function [dydt] = system_of_ode(t,y,k_guess,order_guess,p)
%Prelocate and assign variables/parameters
dydt = zeros(5,1);

nitrile = y(1);
acid     = y(2);
amide    = y(3);
h2o      = y(4);
nh3      = y(5);

k1  = k_guess(1);
k1r = k_guess(2);
k2  = k_guess(3);
k2r = k_guess(4);

order_5 = order_guess(1);
order_6 = order_guess(2);
order_7 = order_guess(3);

% Reactions
reaction_1 = k1*acid^p.order_1*nh3^order_5;
reaction_r1 = k1r*amide^p.order_2*h2o^order_6;
reaction_2 = k2*amide^p.order_3;
reaction_r2 = k2r*nitrile^p.order_4*h2o^order_7;

%Balance Nitrile
dydt(1) = (reaction_2 - reaction_r2);

%Balance Acid
dydt(2) = (reaction_r1 - reaction_1);

%Balance Amide
dydt(3) = (reaction_1 + reaction_r2 - reaction_r1 - reaction_2);

%Balance WATER
dydt(4) = dydt(1) - dydt(2);

%Balance AMMONIA
dydt(5) = dydt(2);
end
```

Appendix II: GC-MS analysis of oleic amide

Table 5: GC-MS analysis of oleic amide

Retention time [minutes]	Confidence [%]	Compound [-]
10.905	96	Dodecanamide
11.605	92	Octadecene nitrile
11.7	94	Heptadecenitrile
12.215	96	Palmitoleamide
12.29	95	Hexadecaneamide
13.315	95	9-Octadecene-nitrile
13.95	93	Octadecanamide
14.29	97	Palmitoleamide
14.485	98	Hexadecaneamide
15.72	92	C ₁₃ amide
18.13	94	Oleic amide
18.325	94	Octadecane amide (stearic)
23.425	93	C ₂₂ amide with unsaturated bond

Appendix III: Molecular sieves in the batch reactor

Experiments were conducted using 10 grams of molecular sieves (UOP Type 3A) with 20 grams of oleic amide as starting reactant. The molecular sieves that were used are 0.125 inch rod shaped and have a pore diameter of 3 Å. These sieves were first activated at temperature above 200 °C for at least an hour. The results can be seen in figure 17 at which the amide conversion looks similar as without sieves, but the selectivity towards nitrile is increased in comparison with the acid.

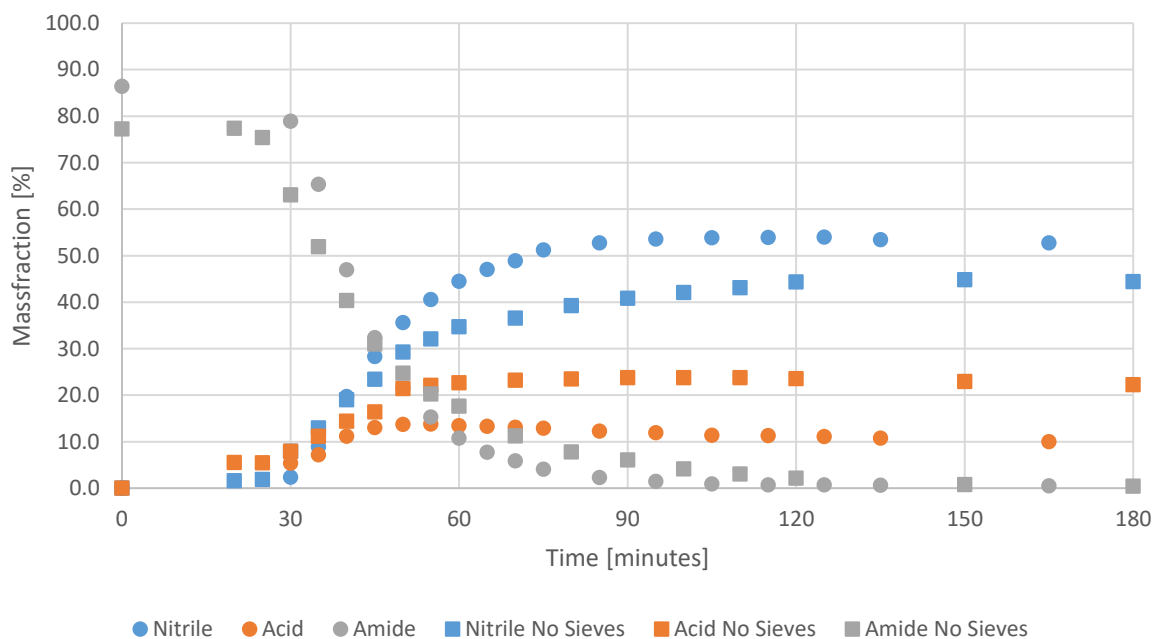


Figure 17: Initial test with molecular sieves